Numerical characterization and flow optimization and heat transfer inside corrugated tubes

Milton Mateush
milton.mateush@tecnico.ulisboa.pt

Instituto Superior Técnico, Universidade de Lisboa, Portugal

October 2021

Abstract

The internal flow in 9 corrugated tubes with pitch ($p = 6, 9, 12\ mm$) and corrugation height ($e = 0.4, 0.5, 0.6\ mm$), regime $Re = 100 - 3000$, was studied in this work to optimize the flow and verify the influence of the corrugation geometry on pressure losses and heat transfer. With water as working fluid and constant heat flux imposed on the tube wall, the $k-\omega$ SST model was used for turbulence. Numerical results demonstrate that corrugation induces a swirl promoting recirculating flow regions which decrease the critical Reynolds number. The thermal performance factor was evaluated and compared to the smooth tube. The best performance for the corrugation geometries was for $Re = 850 - 2300$ where it was verified an almost linear growth. The tube with $p = 6$, $e = 0.6\ mm$ was the best for $Re = 850$, the $p = 12$, $e = 0.5\ mm$ was the best for $Re = 2300$ and the $p = 12$, $e = 0.6\ mm$ was the best in between. For $Re = 100 - 700$ the corrugated tubes show an under-performance compared to the smooth tube. For $Re = 3000$ the performance is similar and doesn't justify the use of a corrugated geometry. A multi-objective optimization study is also performed and it was concluded that for a heat exchanger with the lower pumping power one should use the tube with $p = 6$, $e = 0.6\ mm$ at $Re = 850$ and for maximum thermal performance the $p = 12$, $e = 0.5\ mm$ at $Re = 2300$.
Keywords: internal flow, corrugation height, corrugation pitch, pumping power, thermal performance, heat transfer enhancement, corrugated tubes

1. Introduction

Nowadays there is a great demand of techniques to enhance heat exchanger tubes because they are widely used in applications such as power generation, air conditioning and food industry, among others.

One can use three different techniques to increase the heat transfer in heat exchangers. First there is the active method which requires a power source like a vibrated flow or a surface vibration, second there is the passive method which only depends on a surface modification or extension and finally there is the compound method which is a mix of the two previous or multiple techniques of each method at the same time as rough surface with nano-fluid or fluid vibration.

The main purpose of using passive techniques is to induce swirl and vortices at the secondary flow region, which mix the fluid layers with the core flow and increase the wet area. In this case Kareem [1] explained that the main goal of the corrugation, as similarly said for general passive techniques, is to promote the secondary re-circulation flow by inducing radial velocity components, mixing the flow layers and finally, increasing the wet perimeter with holding the throat cross-section area constant, which leads to an increase of the convective surface area.

Thus, taking into account the parameters previously mentioned, helical inward corrugated tubes (Fig. 1) with different pitch and height will be analyzed in terms of heat transfer and pressure drop for a range of Reynolds number going from laminar to turbulent regime with a final flow optimization study.

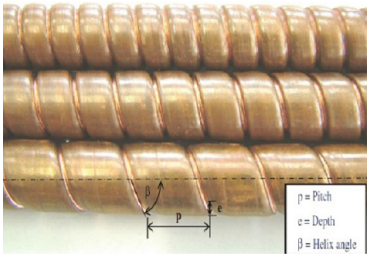

Figure 1: Example of inward helically corrugated tubes with different pitch used by [2]

2. Background

Despite all the circular tube studies, non-circular tubes, especially corrugated tubes, have brought a lot of interest to researchers especially because they involve convection transport and are being more used in compact heat exchangers. In order to compare circular tubes with the helically corrugated ones, an effective diameter (characteristic length) should be defined. Therefore, not only Bergman [3] but also [4, 5, 6] among others, define so this called hydraulic diameter D_h as

$$D_h = \frac{4A_c}{P_{wet}} \tag{1}$$

where A_c is the flow cross section area and P_{wet} corresponds to the wet perimeter of the same. For a circular tube $D_h = D_i = D$.

With this parameter one can redefine the Reynolds number in equation as

$$Re = \frac{u_m D_h}{\nu} \tag{2}$$

The Darcy-Weisbach equation and the Nusselt number equation can also be expressed as

$$f = \frac{2D_h}{\rho u_m^2}\left(\frac{\Delta p}{L}\right) \tag{3}$$

$$Nu = \frac{hD_h}{k} \tag{4}$$

The main parameters that describe the tube are the pitch p and the corrugation height e. For constant exterior and interior diameter, D_e and D_i respectively, and for a certain Re, the pitch and the corrugation height will be the ones to set the flow transition, the heat being transferred and the friction factor associated.

Based on these parameters, researchers tried to find out correlations that could better describe the flow in different regimes inside helically corrugated tubes.

In 2004 Vicente [7, 8] presented two papers. In both of them the results were obtained for $Re' = f(D_i)$ and $Nu' = f(D_i)$. In order to the results to be in agreement with the new equations (2 and 4) outlined for the corrugated tubes, the following conversion can be done, $Re' = (D_i/D_h)Re$ and $Nu' = (D_i/D_h)Nu$, so that the correlations proposed can be $Re = f(D_h)$ and $Nu = f(D_h)$.

So the first paper Vicente [8] was an experimental investigation about laminar and transition flow at 10 horizontal helically corrugated tubes, where water and ethylene glycol were used as test fluids. From their work they came out with a laminar flow friction factor correlation that can be expressed as

$$f = 119.6(Re')^{-0,97}\phi^{0,11} \tag{5}$$

where the equation was multiplied by 4 in order to agree with the Darcy friction factor. That happens because Vicente [8] presented their results on Fanning friction factor basis. In this equation ϕ represents a dimensionless factor called severity index factor which can be defined as

$$\phi = \frac{e^2}{pD_i} \tag{6}$$

So the severity index factor relates the parameters described above and at the same time, it establishes how roughness can influence the flow. It is said that equation 5 correlates 95% of the experimental data within 5% and that for a certain ϕ the friction factor increased between $5 - 25\%$.

At [8] it was also determined a critical Reynolds number based on the study of 10 corrugated tubes leading to the following correlation

$$Re'_{crit} = 2100\left[1 + 1.18 \cdot 10^7\left(\frac{e}{D_i}\right)^{3.8}\right]^{-0.1} \tag{7}$$

which has a 15% accuracy on its values.

For the heat transferred, a Nusselt number correlation was also determined. However, in vicente2004mixed, the flow had a mixed convection heat transfer where the Nusselt number depended not only on the natural convection but also on the entry region, and in this work, heat transferred by forced convection is predominant.

In the second paper Vicente [7] also made an experimental research about the same 10 horizontal hellically corrugated tubes with the same test fluids and flow conditions of $Re' = 2000 - 90000$ and $Pr = 2.5 - 100$. The purpose of this work was to obtain the heat transfer and isothermal friction characteristics of the tubes. From all the tubes tested, 600 points were correlated to experimentally determine the following generalized friction factor correlation for a turbulent flow

$$f = 6.12(Re')^{-0.16}\phi^{0.46} \tag{8}$$

which has a 7% deviation for 95% of the experimental friction data for $Re' = 8000 - 60000$. Once again, the obtained friction factor was multiplied by 4 to be in agreement with the Darcy friction factor. For $Re' = 2000 - 8000$ [7] recommend that equation 8 should only be used for tubes of $\phi < 10^{-3}$ (soft corrugation). For the case that $\phi > 10^{-3}$ (medium-high corrugation) a constant friction factor evaluated with 8 at $Re' = 8000$ should be used. By following these recommendations make estimated error stay within $\pm 10\%$. It is also said that equation 8 can still be used for $Re' > 60000$ however the predicted friction factor values will be 16% higher than the experimental ones.

For the heat transfer results, 800 points were also experimentally correlated to obtain the following generalized Nusselt number correlation for a turbulent flow

$$Nu' = 0.3741(Re' - 1500)^{0.74}\phi^{0.25}Pr^{0.44} \quad (9)$$

which is valid for $Re' > 2000$ and correlates 95% of the empirical data within 14% deviation.

There is not much research made in the laminar regime so this part lacks of correlations.

3. Implementation

Using the 3D CAD modeling software available by STAR-CCM+ [9] it was possible to create 9 geometries for the corrugated tubes and one for the smooth tube for comparison. Only the flow region inside the tubes was considered for the domain. As $D_e = 5$ mm and $D_i = 4.5$ mm were the outer and the inner diameter used for the tubes in this study (the same diameters as Cruz [10] used) the wall thickness of the tubes was neglected. In this case, in order to create the corrugated tubes, the cross section was drawn at first. After that the section was revolved 360 degrees with a sweep command through a guiding line that has the length of the pitch. As the tubes geometry repeats itself every pitch (periodic conditions), the length of the tube is always the same size of the pitch considered. The pitches considered in this study (6, 9, and 12 mm) can be changed by changing the guide line length.

Now considering the corrugation heights used in the tubes (0.4 mm, 0.5 mm and 0.6 mm) one can easily change their value by changing the middle point's height of the spline used to build the cross section. So knowing this, the corrugations used in this study were created to be similar to the ones used by Cruz [10] in order to compare results.

After completing the CAD models, table 1 was made to summarize the most important properties of the tubes that will be analyzed. Note that for numerical purposes only one smooth tube was created (6 mm long).

As it is possible to see the first two columns show the pitches and corrugation heights used. Cruz [10] did numerical and experimental studies with helical inward corrugated tubes with the same pitch variation and from his work he concluded that the pitch had not major influence on the flow transition and that the corrugation height is way more important in this aspect. So that is one of the reasons why this parameter will also be studied in here, because it it important to verify how the transition varies.

In the third and fourth column of table 1 there is the wet area and the wet volume respectively per unit length. As already known, being the corrugation a passive enhanced heat transfer method, the wet areas of the corrugated tubes (for the same pitch) are always greater than the one of the smooth tube. However there is an exception for the tube 7 where the wet area is slightly lower than the smooth tube which happens due to low inward corrugation (0.4 mm). This only means that the corrugation height should have a greater value yet, tube 7 will still be analyzed this way so it can be compared to the other tubes in order to verify if this case is really worth it in terms of heat transfer enhancement.

Now for the wet volume per unit length, it is clear that as the corrugation is placed inward there is less wet volume on the corrugated tubes compared to the smooth tube.

The corrugated tube to smooth tube volume ratio was also studied. So being the smooth tube's wet volume the maximum volume that one tube can have, as higher the corrugation the less is the ratio for the corrugated tubes. This ratio values only depend on the corrugation height and for the corrugation heights of 0.4 mm, 0.5 mm and 0.6 mm the tubes have less 4.06%, 4.74% and 5.42% in wet volume respectively.

In the sixth and seventh columns of table 1 there are the wet perimeter and the cross section area respectively. Both of them only depend on the corrugation height as well and they are always lower than the the smooth tube's perimeter and cross section.

Finally, in the fifth and the three last columns there are the hydraulic diameter (determined with equation 1), the p/D_h and e/D_h adimensional ratios and the severity index (determined with 6) respectively, which can be replaced in the empirical correlations 5, 8 and 9, to obtain the different friction factors and Nusselt numbers for different flow regimes in order to validate the numerical results.

Note that A_w, V_w, P_w and A_c values were are obtained from the CAD models designed on the Star-CCM+ software [9].

The mesh was then defined. The polyhedral mesher, the prism layer mesher and the surface remesher were the models used. Since the corrugated tubes have part of the shape of a smooth tube the generalized cylinder meshing model was also supposed to be chosen. However, since the corrugation heights used in the tubes are too prominent this model did not work as expected and was rejected, especially because every mesh created with this model was an irregular mesh. So for the polyhedral meshing model it is known that it uses an arbitrary polyhedral cell shape to build the core of the mesh. A volumetric control was also created to reduce the number of cells in middle once the most important region for analysis is the region near to the wall.

As the polyhedral mesher is used with a periodic interface, the mesher produce a conformal mesh for

Table 1: Corrugated tubes and smooth tube properties

	$p \cdot 10^3(m)$	$e \cdot 10^3(m)$	$A_w/l \cdot 10^6(m)$	$V_w/l \cdot 10^9(m^2)$	$D_h \cdot 10^3(m)$	$P_w \cdot 10^3(m)$	$A_c \cdot 10^6(m)$	p/D_h	e/D_h	ϕ
tube 1	6	0.4	1.4518E-2	1.5259E-5	4.369	13.971	15.259	1.3734	0.0916	0.0059
tube 2	6	0.5	1.4771E-2	1.5150E-5	4.329	13.998	15.150	1.3859	0.1155	0.0093
tube 3	6	0.6	1.5053E-2	1.5043E-5	4.283	14.050	15.043	1.4010	0.1401	0.0133
tube 4	9	0.4	1.4232E-2	1.5259E-5	4.369	13.971	15.259	2.0601	0.0916	0.0040
tube 5	9	0.5	1.4374E-2	1.5150E-5	4.329	13.998	15.150	2.0789	0.1155	0.0062
tube 6	9	0.6	1.4547E-2	1.5043E-5	4.283	14.050	15.043	2.1015	0.1401	0.0089
tube 7	12	0.4	1.4122E-2	1.5259E-5	4.369	13.971	15.259	2.7468	0.0916	0.0030
tube 8	12	0.5	1.4218E-2	1.5150E-5	4.329	13.998	15.150	2.7719	0.1155	0.0046
tube 9	12	0.6	1.4344E-2	1.5043E-5	4.283	14.050	15.043	2.8020	0.1401	0.0067
smooth tube	-	-	1.4138E-2	1.5904E-5	4.5	14.137	15.904	-	-	-

the periodic boundary pair.

The prism layer mesher is used to generate orthogonal prismatic cells next to the boundaries or wall surfaces creating a layer of cells essential to improve the accuracy of the flow solution. It is defined in terms of its thickness and the number of cell layers within it. Finally, there is the surface remesher which in order to improve the overall quality of the existing surface and optimize it for the volume mesh models, it retriangulates the surface of the geometry.

Note that in the interface the prism layer mesh has an irregular representation however in the interior of the tube it was generated as expected. This irregularities does not compromise the final results.

3.1. Physics models

After defining the mesh, the physics models were chosen to initiate the numerical simulations. However, as the real case studies sometimes are too complex to define, some assumptions were made in order to simplify the numerical studies. The assumptions chosen for this study were water as working fluid, constant water properties evaluated at $300K$, mean bulk inflow temperature of $300K$, incompressible flow, Newtonian fluid (constant viscosity), hydrodynamically and thermically fully developed flow, constant wall heat flux of 100 kW/m^2 and negligible water vaporization ,gravitacional forces and heat transferred by conduction and radiation.

3.2. Laminar, Transition and Turbulent Regime Assumptions

With these assumptions the numerical physics models were then chosen. For the laminar regime the models used where the three dimensional, liquid, segregated flow, constant density, gradients, laminar, steady/implicit unsteady, segregated fluid temperature or isothermal, solution interpolation. and in the other hand, for the turbulent regime the models used were three dimensional, liquid, segregated flow, gradients, constant density, implicit unsteady, turbulent, Reynolds-Averaged Navier-Stokes, all y^+ wall treatment, $k-\omega$ turbulence, SST (Menter) $k-\omega$, wall distance, segregated fluid temperature or isothermal and solution interpolation.

The transition region was considered to occur instantaneously, being only chosen for the different Reynolds numbers a laminar or a turbulent model. It is worth noting that the critical transition Reynolds number for the different corrugated tubes was determined through equation 7 in order to choose the flow regime.

3.3. Verification and Validation

As said by Versteeg [11] one should recognize that errors and uncertainty are inevitable aspects of CFD modelling so it becomes essential to develop rigorous methods to quantify the level of confidence in its results. So in one hand there is the numerical verification which can be defined as the process of determining whether the model implementation accurately represents the developer's conceptual description of the model and the solution to the model. In the other hand there is the numerical validation that can be defined as the process of determining the degree to which a model is an accurate representation of the real world from the perspective of the intended uses of the model.

For the numerical verification a grid independence study was made. The analysis were performed for the worst case scenario, which means, for the tube of lowest pitch and highest corrugation ($p = 6\ mm$ and $e = 0.6\ mm$).

In order to validate the physical models a basic smooth tube problem was evaluated and compared with the available correlations.

4. Results

With the corrugated tubes validation the obtained results are compared to the smooth tube and the optimum working conditions will be described for the tubes with 6 mm pitch and 0.4, 0.5 and 0.6 mm corrugation height, for the tubes with 9 mm pitch and 0.4, 0.5 and 0.6 mm corrugation height and at last for the tubes with 12 mm pitch and 0.4, 0.5 and 0.6 mm corrugation height. Note that all the studies were performed for $Re = 100 - 3000$. Also note that a different nomenclature from Table 1 in the following sections is used in order to be more

clear which tubes are being analyzed in graphs. In the work of Cruz [10], in order to distinguish the different tubes, the severity index (equation 6) was used instead. This approach was not chosen due to very similar severity index values which could induce some confusion.

It was considered an instantaneous transition region for all the tubes were the critical Reynolds number for the onset of the transition region was determined through correlation 7 given by [8]. This correlation confirms that the main parameter responsible for the advance or delay of the onset of the transition region in the corrugated tubes is the corrugation height. The determined critical Re for the 3 different corrugation heights (0.6, 0.5 and 0.4 mm) with 15% accuracy are $\approx$ 753, $\approx$ 807 and $\approx$ 879 respectively (lower margin). It is very clear that the higher the corrugation the lower the critical Reynolds. However, as the values are very similar and in order to ease the analysis the transition region was then defined for the range of Reynolds $Re = 700 - 850$. This range is acceptable once [10], through empirical analysis for the tubes with $e = 0.4\ mm$, determined that the transition range was given by $Re = 850 - 1000$ mentioning that it could even be extended to $Re = 700 - 1100$ to better fit some numerical results.

So for these conditions the following results are presented.

4.1. f vs Re

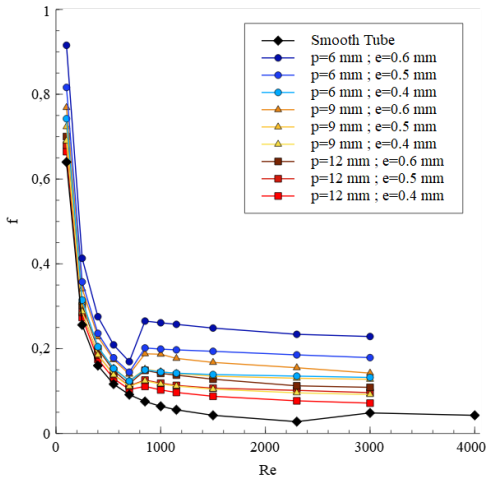

Figure 2: Comparison of the friction factor as function of Reynolds number for the different corrugated tubes and smooth tube

As previously described all the data was analysed for a Reynolds range of $Re = 100 - 3000$. At Fig.2 it is possible to observe a general view of the isothermal friction factor for the different corrugated tubes compared to the smooth tube for the full range. Note that a result for $Re = 4000$ was presented for the smooth tube once its transition region ends at $Re = 3000$ and otherwise there wouldn't be any values for the turbulent regime represented on the chart.

Having a closer look to the laminar region $Re = 100 - 700$ is it possible to confirm that all the corrugated tubes have a higher isothermal friction factor than the smooth tube being the tube with $p = 6\ mm$ and $e = 0.6\ mm$ the worst of all and the smooth tube the best. All the tubes represent the same downtrend having the highest values at a lower Re and then decreasing as we approach the transition region.

Now regarding the turbulent region $Re = 850 - 3000$ one can realize that after the transition ($Re = 700 - 850$) all the tube had an increase in the friction factor values, especially the ones with a higher corrugation height and lower pitch slightly decreasing as the Re in the turbulent region grows.

4.2. Friction Augmentation Factor

After the qualitative analysis one can make a quantitative one through the friction augmentation factor comparison with the smooth tube. In the figure below (Fig.3) it is possible to observe the general view for all the tubes for the friction augmentation factor throughout all the flow regimes.

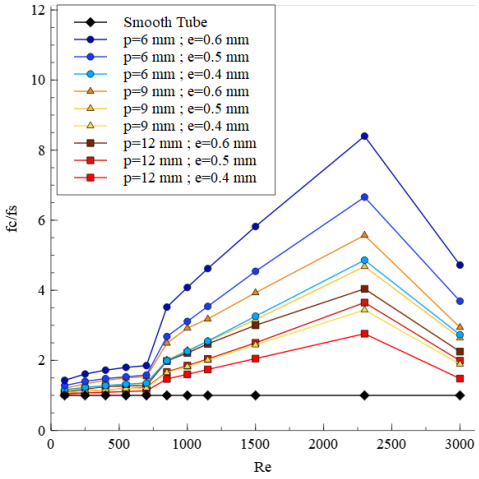

Figure 3: Comparison of the friction augmentation factor as function of Reynolds number for the different corrugated tubes and smooth tube

Having a closer look on the laminar and transition region one can verify that the tube with $p = 12\ mm$ and $e = 0.4\ mm$ has the closest friction values to the smooth tube having an augmentation factor of 1.04 at $Re = 100$ and 1.13 at $Re = 700$. In the other hand the tube with $p = 6\ mm$ and $e = 0.6\ mm$ has the highest friction values for this region compared to the smooth tube, having an augmentation factor of 1.43 at $Re = 100$ and 1.85 at

$Re = 700$. As the transition occurs, either the tube with $p = 12\ mm$ and $e = 0.4\ mm$ and the tube with $p = 6\ mm$ and $e = 0.6\ mm$ increase their friction augmentation values to 1.47 and 3.52 respectively for $Re = 850$.

For the turbulent regime (Fig.3) one can observe that the friction augmentation factor starts to increase more rapidly, practically in a linear way, obtaining its maximum of 8.4 at $Re = 2300$ for the tube with $p = 6\ mm$ and $e = 0.6\ mm$ and for the same Re its lowest of 2.76 for the tube with $p = 12\ mm$ and $e = 0.4\ mm$. It is clear that as soon as the smooth tube becomes turbulent the friction augmentation factor gets very low for all the tubes, becoming 4.72 for the tube with $p = 6\ mm$ and $e = 0.6\ mm$ and 1.48 for the tube with $p = 12\ mm$ and $e = 0.4\ mm$. This happens due to the increase of the isothermal friction factor for the smooth tube for this region.

4.3. Nu vs Re

Now, at Fig.4 it is possible to observe a general view of the average Nusselt number for the different corrugated tubes compared to the smooth tube for the full range. Note that a result for $Re = 4000$ was presented for the smooth tube once its transition region ends at $Re = 3000$ and otherwise there wouldn't be any values for the turbulent regime represented on the chart.

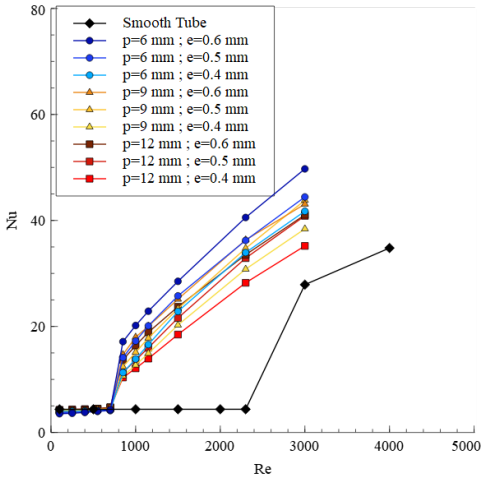

Figure 4: Comparison of the Nusselt number as function of Reynolds number for the different corrugated tubes and smooth tube

Having a closer look to the laminar region $Re = 100 - 700$ it is possible to confirm that all the corrugated tubes have in general a lower average Nusselt number than the smooth tube (opposite to what happened to the isothermal friction factor) being the tube with $p = 6\ mm$ and $e = 0.6\ mm$ again the worst of all.

It is known that in the laminar regime the smooth tube allows a constant heat transfer through the walls (constant Nusselt number) while for the corrugated tubes, they tend to have an uptrend, having the tubes lower Nu values than the smooth tube until $Re \approx 300$ and then slightly higher values until the end of the laminar region at $Re = 700$ where the tube with $p = 12\ mm$ and $e = 0.6\ mm$ has the heighest Nu value.

Now regarding the turbulent region $Re = 850 - 3000$ one can realize that after the transition ($Re = 700 - 850$) all the tubes had an increase in the average Nusselt number, especially the ones with a higher corrugation height and lower pitch.

4.4. Nusselt Augmentation Factor

So in the same way, after the qualitative analysis one can make a quantitative one through the Nusselt augmentation factor comparison with the smooth tube. At Fig. 5 it is possible to observe the general view for all the tubes for the Nusselt augmentation factor throughout all the flow regimes.

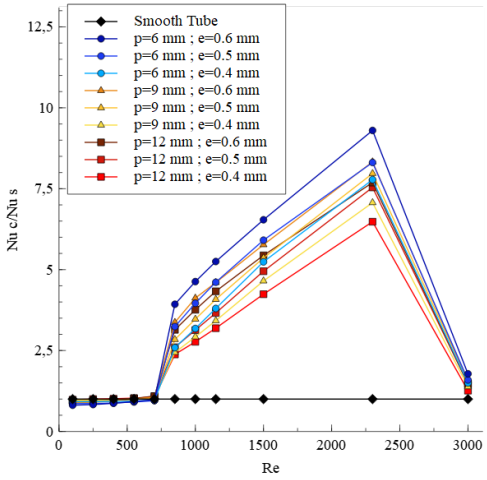

Figure 5: Comparison of the Nusselt augmentation factor as function of Reynolds number for the different corrugated tubes and smooth tube

Having a closer look on the laminar and transition region one can verify that in general all the corrugated tubes similar but slightly lower values of Nu augmentation factor compared to the smooth tube. The tube with $p = 6\ mm$ and $e = 0.6\ mm$ has the lowest augmentation factor for this region, having an augmentation factor of 0.81 at $Re = 100$ and 0.98 at $Re = 700$. As already seen, for some of the corrugated tubes, for $Re > 300$, the Nu augmentation factor has an improvement but still very close to the smooth tube's heat transfer capability. So for $Re = 700$ (at the end of the laminar region) the tube with $p = 12\ mm$ and $e = 0.6\ mm$ obtains the maximum augmentation of 1.09.

As the transition occurs, the tube with $p = 6\ mm$ and $e = 0.6\ mm$ becomes the one with the highest Nu augmentation factor, with 3.93 at $Re = 850$ and the tube with $p = 12\ mm$ and $e = 0.4\ mm$ becomes the worst with a Nu augmentation factor of 2.38 for $Re = 850$. All the tubes have a better performance than the smooth tube after the transition.

For the turbulent regime (Fig.5) one can observe that the Nusselt augmentation factor starts to increase more rapidly, practically in a linear way (the same way that happened to the friction augmentation factor for this regime), obtaining its maximum of 9.3 at $Re = 2300$ for the tube with $p = 6\ mm$ and $e = 0.6\ mm$ and for the same Re its lowest of 6.48 for the tube with $p = 12\ mm$ and $e = 0.4\ mm$. It is clear that as soon as the smooth tube becomes turbulent the Nusselt augmentation factor gets very low for all the tubes, becoming 1.78 for the tube with $p = 6\ mm$ and $e = 0.6\ mm$ and 1.26 for the tube with $p = 12\ mm$ and $e = 0.4\ mm$. This happens due to the increase of the average Nusselt number for the smooth tube for this region.

4.5. Corrugation effect on the flow

Based on the previous analysis one can now discuss and characterize the flow effects that the corrugation causes to the corrugated tubes. The tube with $p = 6\ mm$ and $e = 0.6\ mm$ was used as an example.

As already mentioned by Liebenberg [12] the main purpose of using passive techniques is to induce swirl and vortices at the secondary flow region which will mix the fluid layers with the core flow and increase the wet area. Kareem [1] also stated that the main goal of the corrugation is to promote the secondary re-circulation flow by inducing radial velocity components, mixing the flow layers and finally, increasing the wet perimeter with holding the throat cross-section area constant, which leads to an increase of the convective surface area. Therefore, the induced swirl effect it is pointed as the main feature of the corrugated tubes. As mentioned by Cruz [10], this effect is however mostly characterized by experimental results where its hard to analyse and obtain a qualitative description of the resulting flow.

As per numerical analysis made for the different corrugated tubes, one can affirm that the swirl effect produced by the corrugation transforms the inlet axial flow into a 3 dimensional flow which is decomposed into the 3 dimensional components of the velocity in cylindrical coordinates (axial, radial and tangential respectively). The influence on the corrugated tubes can then be verified on the pressure losses and heat transfer through the tubes.

Starting by the axial velocity component, one can say that the velocity profile shows a similar behaviour to the smooth tube. As mentioned by Cruz [10], the continuity equation and the wall boundary condition (no-slip condition) forces the mass flow to the center of the tube, accelerating the flow towards the center. The same behaviour was verified for the laminar and turbulent region. Note that the tube with $p = 6\ mm$ and $e = 0.6\ mm$ was only chosen as an example.

Now for the radial velocity component, it is known to have its origin due to the corrugation geometry. As this work analysis and Cruz [10], close to the corrugation, there is a zone where the flow has a radial negative component of the velocity. In his work it was also referred that its magnitude is almost 10 times higher than the rest of the tube's section. In this case, for the tube with $p = 6\ mm$ and $e = 0.6\ mm$, the magnitude is ≈ 6 times higher for the laminar region and and ≈ 7 times higher for the turbulent region. This radial velocity magnitude is very small when compared with the magnitudes that the axial component of the velocity assumes. Therefore, and as per [10], it can be concluded that this radial component, despite being clearly produced by the corrugation, it is not large enough to, by itself, affect the flow significantly.

Finally, for the tangential velocity component, one can say that it induces swirls around the tube walls to towards the corrugation. At [10] it is said to have a maximum magnitude is 10% of the axial component magnitude. In this case for the tube with $p = 6\ mm$ and $e = 0.6\ mm$, the maximum tangential magnitude compared to the axial one is $\approx 11\%$ for the laminar region and and $\approx 30\%$ for the turbulent region. Therefore, the effects of the corrugation in the tangential velocity component are definitely more significant than in the radial one.

4.6. Thermal Performance

In the previous sections the isothermal friction factor (resultant of the pressure drop determined for each tube) and the average Nusselt number (heat transferred by each tube) were the two parameters that were studied and compared to the smooth tube's numerical data. Both of them were individually qualitatively and quantitatively analysed with the the support of the friction and Nusselt augmentation factors respectively. However an analysis which involves the combination of these two parameters is also needed. So based on this and in order to achieve this dual criteria analysis the thermal performance factor presented in equation 10 below can be used.

$$\eta = \frac{Nu_c/Nu_s}{(f_c/f_s)^{1/3}} \tag{10}$$

This equation defines the ratio of the enhanced tube heat transfer coefficient to the smooth tube at constant pumping power and it was used by Wang [6] and Pethkool [13] among others.

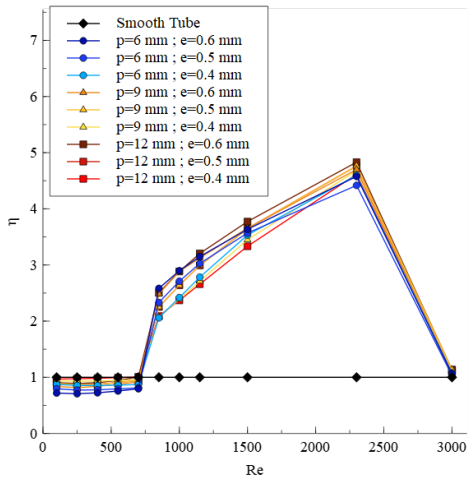

Figure 6: Comparison of the thermal performance as function of Reynolds number for the different corrugated tubes and smooth tube

Being this said, in the figure Fig. 6, it is possible to observe the general view for all the tubes for the Thermal Performance factor as function of Re throughout all the flow regimes ($Re = 100 - 3000$).

Looking closer to the laminar region ($Re = 100 - 700$), one can verify that all the corrugated tubes have a worse thermal performance than the smooth tube. This can be explained by the fact that for this regime the corrugation works more as an obstacle then as a heat transfer enhancement technique which makes the corrugation tubes have a higher friction factor than the smooth tube (Fig.2) and a lower heat transfer comparing to the same (Fig.4).

As it is possible to see the values are slightly lower then the smooth tube's, being the tube with $p = 6\ mm$ and $e = 0.6\ mm$ the lowest performance for this region, having a factor of 0.72 at $Re = 100$ and 0.8 at $Re = 700$. The tube with $p = 12\ mm$ and $e = 0.4\ mm$ has the closest thermal performance to the smooth tube, having a factor of 0.97 at $Re = 100$ and 1.01 at $Re = 700$. This happens due to the fact that this corrugated tube has a low corrugation height and therefore the closest wet area per unit length to the smooth tube's (Table 1).

As the transition occurs ($Re = 700 - 850$) there is a boost in thermal performance and the tube with $p = 6\ mm$ and $e = 0.6\ mm$ becomes the one with the highest thermal performance factor, 2.58 for $Re = 850$, and the tube with $p = 6\ mm$ and $e = 0.4\ mm$ becomes with the one with the lowest value, 2.06 for $Re = 850$. So all the corrugated tubes have a better performance than the smooth tube after the transition.

For the turbulent regime presented at Fig.6 ($Re = 850 - 3000$) one can observe that the thermal augmentation factor starts to increase more rapidly, practically in a linear way (the same behaviour as the friction augmentation factor and Nusselt augmentation factor for this regime), obtaining its maximum of 4.9 at $Re = 2300$ for the tube with $p = 12\ mm$ and $e = 0.5\ mm$ and for the same Re its lowest of 4.42 for the tube with $p = 6\ mm$ pitch and $e = 0.5\ mm$. In the middle section, for Reynolds between 850 and 2300 the tube with $p = 12\ mm$ and $e = 0.6\ mm$ prevails with the highest thermal performance factor. There is such high thermal performance factor values in this range once the smooth tube is still in the laminar region and due to secondary flow resulting from vorticity.

Looking closer at the turbulent region it is clear that as soon as the smooth tube becomes turbulent (from $Re = 3000$) the thermal performance factor gets very low for all the corrugated tubes, having a maximum of 1.17 at $Re = 3000$ for the tube with $p = 12\ mm$ and $e = 0.5\ mm$ and having a minimum of 1.03 at $Re = 3000$ for the tube with $p = 6\ mm$ and $e = 0.5\ mm$. As already mentioned this happens due to the increase of the heat transfer for the smooth tube for this region.

In conclusion, for laminar region $Re = 100 - 700$ the thermal augmentation factor tends to be slightly lower for all the tubes. As the transition for the corrugated tubes occur there is a jump in the thermal performance which grows almost linearly for all the cases in the range of $Re = 850 - 2300$. Then, when the smooth tube becomes turbulent $Re = 2300 - 3000$ all the thermal performance factors decrease becoming almost as low as the laminar ones.

Comparing this results with the ones obtained by Cruz [10] one can say that the thermal performance chart from his study demonstrate the same behaviour of the one here presented. However, one should note that for the laminar thermal performance factor, the results presented by his work are very high and better than the smooth tubes ones which can be explained by the fact that in his experimental work it was not possible to obtain thermally fully developed conditions for the laminar region. In his work he also defines the region with the best thermal performance which goes from $Re = 1000$ (post corrugation tube transition) to $Re = 2000$ (pre smooth tube transition) and in fact it corresponds to the same here obtained ($Re = 850 - 2300$). In the turbulent regime he also presented lower values of thermal performance factor being those similar to the ones determined for the laminar regime.

4.7. Pareto Efficiency Curve

Once the data from the thermal performance factor it is not enough to characterize the optimum flow working conditions for a heat exchanger it was also performed a multi-objective optimization study which determined the Pareto efficiency presented at Fig.7. This study has the aim to verify the working conditions where it is possible to minimize the volume per heat transferred across the wall while minimizing pumping power.

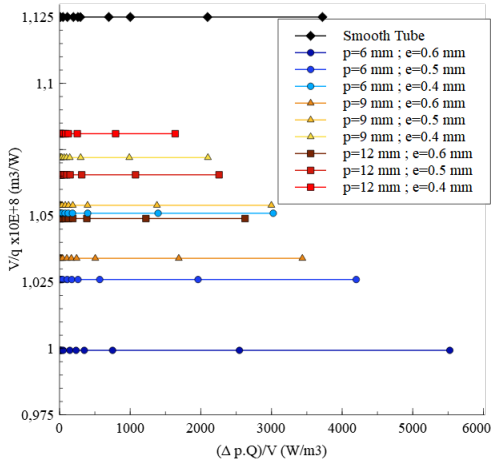

Figure 7: Pareto efficiency curve for the different corrugated tubes and smooth tube

As the heat flux through the walls of the different tubes is constant, the heat transferred is also constant. With a constant wet volume for each tube, in the chart one can observe horizontal lines once the volume per heat transferred (y axis) ends up being also constant which means that it is independent of the pumping power per unit volume (x axis).

So based on the results on Fig.6 where it was concluded that the best thermal performance is achieved in the range $Re = 850 - 2300$ and based on the Fig.7 where it is intended to minimize the volume per heat transferred across the wall while minimizing pumping power, it is possible to affirm that the most efficient working conditions happen for the tube with $p = 6\ mm$ and $e = 0.6\ mm$ for $Re = 850$. In case the best thermal performance is needed the tube with $p = 12\ mm$ and $e = 0.5\ mm$ for $Re = 2300$ can be chosen at a cost of a higher pumping power and higher volume per heat transferred.

Note that a higher pumping power implies a higher Reynolds number (along the x axis) being the last three dots to the right (of each curve) the pumping power corresponding to $Re = 1500$, 2300 and 3000 respectively. The lower Reynolds numbers ($Re = 100 - 1150$) dots are almost all together (for each curve) near to the y axis (volume per heat transferred) requiring then a lower pumping power. Being more precise, the highest pumping power for the laminar regime ($Re = 100 - 700$) goes for the corrugated tube with $p = 6$ and $e = 0.6\ mm$ with a value of 52 W/m^3 for $Re = 700$. The lowest pumping power for the laminar regime goes for the corrugated tube with $p = 12\ mm$ and $e = 0.4\ mm$ with a value of 30.1 W/m^3 for $Re = 700$. Finally, for the turbulent region $Re = 850 - 300$, the highest pumping power the happens again for the corrugated tube with $p = 6\ mm$ and $e = 0.6\ mm$ with a value of 5524.1 W/m^3 for $Re = 3000$ and the lowest pumping power the happens again for the corrugated tube with $p = 12\ mm$ and $e = 0.4\ mm$ with a value of 1637 W/m^3 for $Re = 3000$.

One can also observe that the smooth tube has similar values of pumping power to the tube with $p = 9\ mm$ and $e = 0.6\ mm$ however its volume per heat transferred is higher than all the other corrugated tubes. Despite this value being higher for the smooth tube, in general, in terms of magnitude they are all very close varying main in the pumping power which has an almost exponential growth as the Reynolds number increase.

5. Conclusions

The following main conclusions can be presented:

- Corrugation induces a swirl promoting recirculating flow regions which decrease the critical Reynolds number and anticipate onset of the transition region and a higher corrugation height implies a faster transition;

- Thermal hot-spots with pulsating thermal behaviour were identified along a periodic corrugated tube domain;

- The best performance for the corrugation geometries was for $Re = 850 - 2300$ where it is verified an almost linear growth. The tube with $p = 6\ mm$ and $e = 0.6\ mm$ was the best in terms of thermal performance factor for $Re = 850$ with a value of 2.58, the tube with $p = 12\ mm$ and $e = 0.5\ mm$ was the best for $Re = 2300$ with a value of 4.9 and the tube with $p = 12\ mm$, $e = 0.6\ mm$ was the best in between. For $Re = 100 - 700$ the corrugated tubes show a lower thermal performance compared to the smooth tube and therefore it doesn't justify the use of a corrugated geometry. For $Re = 3000$ the thermal performance is similar and also doesn't justify the use of a corrugated geometry;

- For constant heat flux and wet volume for each tube the heat transferred across the wall becomes constant and independent of the pumping power;

- In order to the heat exchanger to work with improved thermal performance and lower pumping power one should use the tube with $p = 6\ mm$ and $e = 0.6\ mm$ at $Re = 850$. To work with the maximum thermal performance one should use the tube with $p = 12\ mm$, $e = 0.5\ mm$ at $Re = 2300$ with a cost of a higher pumping power and a higher volume per transferred heat.

5.1. Recommendation for Future Work

The following points are presented:

- Expand the analysis for higher Reynolds numbers ($Re > 3000$) once the smooth tube's transition occurs very late and improve the numerical analysis (better convergence);
- Redo the experimental analysis for the 3 tubes with 6, 9 and 12 mm pitch and 0.4 mm corrugation height and make experimental analysis for the 3-off tubes with 6, 9 and 12 mm pitch and 0.5 mm corrugation height and the 3 tubes with 6, 9 and 12 mm pitch and 0.6 mm in fully developed hydrodynamic and thermal conditions in order to allow a better numerical results validation;
- Test the corrugated tubes in comparison with the smooth tube with a different test fluid (different Prandtl number) and test the corrugated tubes in comparison with the smooth tube with the constant wall temperature boundary condition instead of constant heat flux;
- Develop a double heat pipe heat exchanger or a compact heat exchanger made with the different corrugated tubes in order to evaluate the thermal performance and pumping power impact, both numerically and experimentally;

References

[1] Zaid S Kareem, MN Mohd Jaafar, Tholudin M Lazim, Shahrir Abdullah, and Ammar F Abdulwahid. Passive heat transfer enhancement review in corrugation. *Experimental Thermal and Fluid Science*, 68:22–38, 2015.

[2] Suriyan Laohalertdecha, Ahmet Selim Dalkilic, and Somchai Wongwises. Correlations for evaporation heat transfer coefficient and two-phase friction factor for r-134a flowing through horizontal corrugated tubes. *International communications in heat and mass transfer*, 38(10):1406–1413, 2011.

[3] Theodore L Bergman, Frank P Incropera, David P DeWitt, and Adrienne S Lavine. *Fundamentals of heat and mass transfer*. John Wiley & Sons, 2011.

[4] Chen Yang, Gan Liu, Junhui Zhang, and Jinyuan Qian. Thermohydraulic analysis of hybrid smooth and spirally corrugated tubes. *International Journal of Thermal Sciences*, 158:106520, 2020.

[5] Raheem K Ajeel, W Saiful-Islam, K Sopian, and MZ Yusoff. Analysis of thermal-hydraulic performance and flow structures of nanofluids across various corrugated channels: An experimental and numerical study. *Thermal Science and Engineering Progress*, 19:100604, 2020.

[6] Wei Wang, Yaning Zhang, Kwan-Soo Lee, and Bingxi Li. Optimal design of a double pipe heat exchanger based on the outward helically corrugated tube. *International Journal of Heat and Mass Transfer*, 135:706–716, 2019.

[7] Pedro G Vicente, Alberto Garcıa, and Antonio Viedma. Experimental investigation on heat transfer and frictional characteristics of spirally corrugated tubes in turbulent flow at different prandtl numbers. *International Journal of Heat and Mass Transfer*, 47(4):671–681, 2004.

[8] PG Vicente, A Garcia, and A Viedma. Mixed convection heat transfer and isothermal pressure drop in corrugated tubes for laminar and transition flow. *International Communications in Heat and Mass Transfer*, 31(5):651–662, 2004.

[9] Siemens PLM Software. Star-ccm+ (version 2020.1), 2004.

[10] Gonçalo Jorge Granjal Cruz. Experimental and numerical characterization of the flow and heat transfer inside corrugated pipes. Master's thesis, Instituto Superior Técnico, November 2019.

[11] Henk Kaarle Versteeg and Weeratunge Malalasekera. *An introduction to computational fluid dynamics: the finite volume method*. Pearson education, 2007.

[12] Leon Liebenberg and Josua P Meyer. In-tube passive heat transfer enhancement in the process industry. *Applied Thermal Engineering*, 27(16):2713–2726, 2007.

[13] S Pethkool, S Eiamsa-Ard, S Kwankaomeng, and P Promvonge. Turbulent heat transfer enhancement in a heat exchanger using helically corrugated tube. *International Communications in Heat and Mass Transfer*, 38(3):340–347, 2011.